Exact Floquet states of a driven condensate and their stabilities

Wenhua Hai[1], **Chaohong Lee**[2] **and Qianquan Zhu**[1]

[1]Department of Physics, Hunan Normal University, Changsha 410081, P. R. China
[2]Nonlinear Physics Centre and ARC Centre of Excellence for Quantum-Atom Optics, Research School of Physical Sciences and Engineering, Australian National University, Canberra ACT 0200, Australia

E-mail: whhai2005@yahoo.com.cn (corresponding author), chl124@rsphysse.anu.edu.au

Abstract. We investigate the Gross-Pitaevskii equation which describes an atomic Bose-Einstein condensate confined in an optical lattice and driven by a spatiotemporal periodic laser field. It is demonstrated that the exact Floquet states appear when the external time-dependent potential is balanced by the nonlinear mean-field interaction. The balance region of parameters is divided into a phase-continuing region and a phase-jumping one. In the latter region, the Floquet states are spatiotemporal vortices of nontrivial phase structures and zero-density cores. Due to the velocity singularities of vortex cores and the blowing-up of perturbed solutions, the spatiotemporal vortices are unstable periodic states embedded in chaos. The stability and instability of these Floquet states are numerically explored by the time evolution of fidelity between the exact and numerical solutions. It is numerically illustrated that the stable Floquet states in the phase-continuing region could be prepared from the uniformly initial states by slow growth of the external potential.

PACS numbers: 03.75.Lm, 03.75.Kk, 05.45.Mt, 03.65.Ge

Keywords: Bose-Einstein condensate, exact Floquet solution, periodic state embedded in chaos, spatiotemporal vortex, stability, fidelity

Submitted to: *J. Phys. B: At. Mol. Opt. Phys.*

1. Introduction

The atomic Bose-Einstein condensates (BECs) in optical lattices have stimulated great interests in both the many-body quantum effects [1]-[4] and mean-field dynamics [5]-[7]. It has been suggested for applications in quantum interference [1, 2], quantum information processing [8, 9, 10] and matter-wave manipulation [11, 12]. Using the mean-field theory, some exact stationary solutions for the systems of one-dimensional (1D) optical lattices were obtained [13, 14, 15], and their stabilities are discussed [16, 17]. Some nonstationary states of BECs in time-dependent lattices have also been investigated [18]-[21].

The Floquet states, a kind of nonstationary states, have been extensively introduced to understand the dynamics of various driven systems [22, 23]. For a linear Schrödinger system of T-periodic Hamiltonian, $H(\vec{r},t) = H(\vec{r},t+nT)$, the Floquet theorem allows one to write its states as $\Psi(\vec{r},t) = U(\vec{r},t)\exp(-iE_Ft)$ with periodic function $U(\vec{r},t) = U(\vec{r},t+nT)$ and quasienergy E_F. The Floquet analysis is analogous to the Bloch analysis in solid state physics in which the states of spatially periodic system are written in terms of Bloch states and quasimomenta. Recently, the Floquet analysis has been introduced to systems of condensed atoms. For driven systems of BECs in double-well potentials, applying a two-mode approximation to the Gross-Pitaevskii (GP) equation, the Floquet states have been used to analyze the coherent control of the population self-trapping [22, 23]. For the driven ultracold Bose atoms in optical lattices, which obey driven Bose-Hubbard models in full quantum theory, the Floquet states are applied to investigate the dynamical superfluid-insulator transition [24]. Below, we will generalize the familiar Floquet states in driven linear Schrödinger systems to the ones in a driven nonlinear Schrödinger system without any approximation.

Spatial vortices [25] are fundamental objects of spinning, often turbulent, flow (or any spiral motion) with closed streamlines. They widely exist in different fields including phase singularities in optics [26] and circulating particles in superfluids and BECs [27]. Recently, the conception of vortex in spatial domain has been generalized to the one in spatiotemporal domain. It shows that the superposition of two phase modulated optical beams generates the train of spatiotemporal vortices, which are periodical in space or time [28]. We expect such spatiotemporal vortices can also appear in an atomic BEC under some certain conditions.

The stability analysis can provide useful information for preparation, control and application of a particular state. Mathematically, the instability appears when an initially small deviations do not keep bounded. It has been demonstrated that a blowing-up solution [29] appears in a BEC system and is related to the BEC collapse and instability [30]. For a linear quantum system, the fidelity between the unperturbed and perturbed states, a quantum Loschmidt echo, has been successfully used to analyze the stability [31, 32]. In which, the fast decay of fidelity corresponds to the instability of a quantum evolution. In the following, we will extend such a fidelity analysis to the nonlinear quantum systems of BECs.

In this article, we show how to prepare the exact Floquet states of an atomic BEC trapped in an optical lattice and driven by a spatiotemporally periodic field, and also analyze their stabilities. Utilizing the balance condition between the external potentials and mean-field interaction, we obtain a kind of exact Floquet solutions for the non-integrable chaotic system. The balance region of parameters is divided into the phase-continuing region and phase-jumping one, which are associated with the stable periodic states and unstable spatiotemporal vortex states embedded in chaos respectively. The stability and instability are confirmed by the corresponding fidelities between the exact and the numerical solutions. Our results suggest a method for suppressing the instability and preparing stable non-stationary states of the condensates. The considered condensate stabilization and preparation could be experimentally realizable.

2. Model and exact Floquet states

We consider an atomic BEC with strongly transverse confinement, and so that it obeys a quasi-1D GP equation,

$$i\hbar\psi_t = -\frac{\hbar^2}{2m}\psi_{xx} + [g_{1d}|\psi|^2 + V(x,t)]\psi, \tag{1}$$

where m is the single-atom mass and g_{1d} denotes the quasi-1D interaction strength [33], and $V(x,t)$ stands for the external potential $V(x,t) = V_0\cos^2(kx) + f(x,t)$ with lattice potential $V_0\cos^2(kx)$ of strength V_0 and driving field $f(x,t)$ to be determined, and the wave vector k.

To obtain the exact solutions of model (1) with the balance technique [13, 15], we use the balance condition

$$g_{1d}|\psi|^2 + V(x,t) = E_F \tag{2}$$

with E_F being a constant, which means that the nonlinear mean-field interaction is balanced by the external potential. Subsequently, the model (1) is simplified as

$$i\hbar\psi_t = -\frac{\hbar^2}{2m}\psi_{xx} + E_F\psi \tag{3}$$

whose complete solution which contains some arbitrary constants can be easily obtained [15] and the corresponding integration constants are determined by inserting the complete solution into Eq. (2). Obviously, Eqs. (2) and (3) supports the exact Floquet state,

$$\begin{aligned}\psi(x,t) = &\left[\sqrt{\frac{E_F}{g_{1d}}} + \alpha\sqrt{-\frac{V_0}{g_{1d}}}\cos(kx)e^{-i\omega t}\right] \\ &\times \exp\left(-\frac{i}{\hbar}E_F t\right),\end{aligned} \tag{4}$$

where ω is the driving frequency, E_F is the Floquet energy, $\sqrt{E_F/g_{1d}}$, $\sqrt{-V_0/g_{1d}}$ and $\sqrt{-E_F V_0}$ are real quantities, and α denotes a constant with value being either 1 or -1. In the absence of a potential, $V(x,t) = 0$, the solution has an uniform density distribution

$|\psi|^2 = \mu/g_{1d}$ for $\psi = \sqrt{\mu/g_{1d}}\, e^{-i\mu t}$ with $\mu = E_F$. In the case of $V_0 \neq 0$ and $f = 0$, the balance solution (4) contains the stationary state $\psi(x,t) = \alpha\sqrt{-V_0/g_{1d}}\cos(kx)e^{-i\mu t}$ for the chemical potential $\mu = \omega = \hbar k^2/2m$ and zero Floquet energy $E_F = 0$. In general, the balance condition (2) and Floquet solution (4) require the driving frequency ω and recoil energy E_r of the optical lattice satisfy the relation

$$\hbar\omega = E_r = \frac{\hbar^2 k^2}{2m}, \tag{5}$$

and the driving field has the form

$$f(x,t) = V_1 \cos kx \cos\omega t, \quad V_1 = 2\alpha\sqrt{-E_F V_0}, \tag{6}$$

where the driving strength V_1 is determined by the lattice depth V_0 and the Floquet energy E_F. Given Eq. (5) and the form of potential, the second of Eq. (6) becomes the balance condition corresponding to Eq. (2). This condition indicates the relation between the driving strength V_1 and frequency ω for the requirement of the balance. The real values of $\sqrt{E_F/g_{1d}}$ requires that the attractive ($g_{1d} < 0$) and repulsive ($g_{1d} > 0$) condensates have negative and positive Floquet energies, respectively. The driving field in Eq. (6) is a time-dependent laser standing wave, which can be formed from the linear superposition of two counter-propagating travelling waves [19]. It is clear that the classical system governed by the total potential $V(x,t) = V_0\cos^2 kx + V_1\cos kx\cos\omega t$ is chaotic and non-integrable [34, 35, 36], and the corresponding GP system (1) is also non-integrable chaotic one even for the stationary state case [6].

Starting from the non-stationary states (4), one can selectively prepare different stationary states of expected chemical potential $\mu = \omega$ via selecting the driving frequency ω and adiabatically switching off the driving field, namely decreasing V_1 to zero very slowly. Under the balance condition (6) this adiabatic operation makes $V_1 = 0$ and $E_F = 0$ such that Eq. (4) becomes the simple stationary solution $\psi(x,t) = \alpha\sqrt{-V_0/g_{1d}}\cos(kx)e^{-i\mu t}$ for $\mu = \omega$ and $\alpha = \pm 1$, which still obeys the balance condition (2) and additional Eqs. (3) and (5). It has been demonstrated that such a stationary state which has zero points possesses instability or undetermined stability for $g_{1d} > 0$ or $g_{1d} < 0$ respectively [17]. Different from the stationary states, the exact Floquet state for a driven condensate has a nontrivial phase which cannot be simply decoupled into a spatially dependent part from the super flow and a temporally dependent part dominated by the chemical potential. In contrast, this nontrivial phase includes a spatiotemporally dependent part from the super flow and a temporally dependent part dominated by the Floquet energy. This is resulted from the spatiotemporal dependence of the super flows in driven condensates.

Defining the average number of atoms per well as $N = \int_0^\pi |\psi|^2 d(kx)/k = \pi(E_F - V_0/2)/(kg_{1d})$, the Floquet energy can be expressed as $E_F = kg_{1d}N/\pi + V_0/2$. The real values of $\sqrt{E_F/g_{1d}}$ and $\sqrt{-V_0/g_{1d}}$ in Eq. (4) require $E_F/g_{1d} = kN/\pi + V_0/(2g_{1d}) \geq 0$ and the lattice strength V_0 satisfying,

$$|V_0| \leq V_c = 2kN|g_{1d}|/\pi. \tag{7}$$

Given the E_F and condition $V_0/g_{1d} < 0$, the balance condition in Eq. (6) gives $V_1 = 2\alpha\sqrt{-E_F V_0} = \alpha\sqrt{-2(2kNg_{1d}/\pi + V_0)V_0}$. This formula and Eq. (7) confine the driving field strength

$$|V_1| = \sqrt{2|V_0|(V_c - |V_0|)} \leq V_c/\sqrt{2}, \tag{8}$$

where the inequality is derived from the maximum condition $d|V_1|/d|V_0| = 0$ for a fixed V_c. Therefore, V_c and $V_c/\sqrt{2}$ are the supercritical values of the lattice depth $|V_0|$ and driving strength $|V_1|$ for the balance solution.

Due to $\cos(kx) = \frac{1}{2}(e^{ikx} + e^{-ikx})$, the exact Floquet solution (4) can be regarded as the coherent superposition between an atom standing wave formed by two counter-propagating plane waves and the background $\sqrt{E_F/g_{1d}}\exp(-iE_F t/\hbar)$. Writing the macroscopic wave function as $\psi = R(x,t)\exp[i\theta(x,t)]$, the exact solution (4) implies the atomic-number density

$$\begin{aligned} R^2 &= |\psi|^2 \\ &= \frac{1}{g_{1d}}\left(E_F - V_0\cos^2 kx - V_1\cos kx\cos\omega t\right) \end{aligned} \tag{9}$$

and the phase

$$\begin{aligned} \theta =& \arctan[Im(\psi)/Re(\psi)] \\ =& \arctan\frac{\sqrt{|V_0|}\cos kx\sin\omega t}{\sqrt{|E_F|} + \sqrt{|V_0|}\cos kx\cos\omega t} - \frac{E_F}{\hbar}t. \end{aligned} \tag{10}$$

Clearly, the atomic density $R^2(x,t)$ has the same profile of the potential function and can be controlled by the external fields. The exact formula for the amplitude R and its finite form will raise the control precision. The non-integrability of the system means that its solution cannot contain the integration constants determined by the initial and boundary conditions. Therefore, the general solution cannot be given exactly. Of course, one may write an exact solution in terms of a superposition of an ensemble of complete orthogonal sets including Fourier modes, which could contain infinite terms.

3. Spatiotemporal vortices

It is well known that the vortices are associated with the phase singularities. The phase accumulation along a closed circle around the vortex core and the phase jump along a line through the vortex core are determined by the vortex charge. According to the relation between the phase and the velocity, $\vec{v} = \frac{\hbar}{m}\vec{\nabla}\theta$, the velocity divergence appears when there is phase jump. In our GP system (1), the velocity field is defined as $v = \frac{\hbar}{m}\theta_x$ with

$$\theta_x = \frac{kV_1}{2g_{1d}R^2(x,t)}\sin kx\sin\omega t \tag{11}$$

denoting the first derivative (gradient) of the phase (10). The corresponding flow density $J = R^2\theta_x = \frac{kV_1}{2g_{1d}}\sin kx\sin\omega t$ with amplitude being proportional to the driving strength V_1 describes the Floquet oscillations of the system. Given the density distribution (9),

we know that the macroscopic wave function has zero-density nodes (x_{zd}, t_{zd}) satisfying $R^2(x_{zd}, t_{zd}) = 0$, i.e.,

$$\cos(kx_{zd}) = \frac{-V_1 \cos(\omega t_{zd}) \pm \sqrt{V_1^2 \left[\cos^2(\omega t_{zd}) - 1\right]}}{2V_0}. \tag{12}$$

Because $\cos(kx_{zd})$ are real quantities, one can get

$$\cos(\omega t_{zd}) = \pm 1, \;\; \cos(kx_{zd}) = -\frac{V_1}{2V_0}\cos(\omega t_{zd}) = \pm\frac{V_1}{2V_0}$$

from the above formula. Thus the spatiotemporal coordinates (x_{zd}, t_{zd}) for the zero-density nodes read

$$t_{zd} = t_n = n\frac{\pi}{\omega}, \tag{13}$$

$$x_{zd} = x_{nl}^{\pm} = \frac{1}{k}\left[\pm \arccos\left(\frac{-V_1 \cos n\pi}{2V_0}\right) + 2l\pi\right] \tag{14}$$

with non-negative integers n and l. The phase gradient (11) becomes infinite at those zero-density nodes when $\sin\left(kx_{nl}^{\pm}\right) \neq 0$. The infinite phase gradient $\theta_x(x_{nl}^{\pm}, t_n)$ means that the phase is a step function across the zero-density nodes $(x_{nl}^{\pm}, t_n)$. Using the relation between velocity and phase gradient, we know that the velocity singularity appears at these points. Due to the nonlinear mean-field interactions otherwhere, Eqs. (11) and (9) imply that the velocity singularity at the density nodes with $E_F = V(x_{zd}, t_{zd})$ is an effect of nonlinear resonance [37].

The conditions (8) and $\sin\left(kx_{nl}^{\pm}\right) \neq 0$ which is equivalent to $\cos^2\left(kx_{nl}^{\pm}\right) = \frac{V_1^2}{4V_0^2} < 1$ give the following parametric region,

$$|V_1| < 2|V_0| \quad \textit{and} \quad V_c/3 < |V_0| < V_c, \tag{15}$$

in which phase jumps may occur. In this parametric region, applying the l'Höpital rule to the phase gradient (11), one can find

$$\lim_{t\to t_n} \theta_x(x_{nl}^{\pm}, t) = \pm\frac{k}{2}\lim_{t\to t_n}\left[\tan(kx_{nl}^{\pm})\cot(\omega t)\right] = \infty. \tag{16}$$

However, the time derivative of phase,

$$\lim_{t\to t_n} \theta_t(x_{nl}^{\pm}, t) = \omega/2 - E_F/\hbar \tag{17}$$

keeps finite at $(x_{nl}^{\pm}, t_n)$. This means that the phase jumps occur along the spatial direction but not along the temporal direction. Thus, the whole balance region is divided into two parts with or without phase jumps. The boundary between two parts has $|V_1| = 2\sqrt{|E_F V_0|} = 2|V_0|$, $|V_0| = |E_F| = V_c/3$, $R^2(x_{nl}^{\pm}, t_n) = 0$, $\sin(kx_{nl}^{\pm}) = 0$ and finite $\theta_x(x_{nl}^{\pm}, t_n)$. The latter indicates that the exact Floquet solutions at the boundary are not phase-jump solutions. In the phase-jump region, the driving field strength $|V_1|$ is smaller than two times of the lattice strength $2|V_0|$.

Similarly, applying the l'Höpital rule to the following quantities, one can easily obtain

$$\lim_{t\to t_n} R_x(x_{nl}^{\pm}, t) \propto R(x_{nl}^{\pm}, t_n) = 0,$$

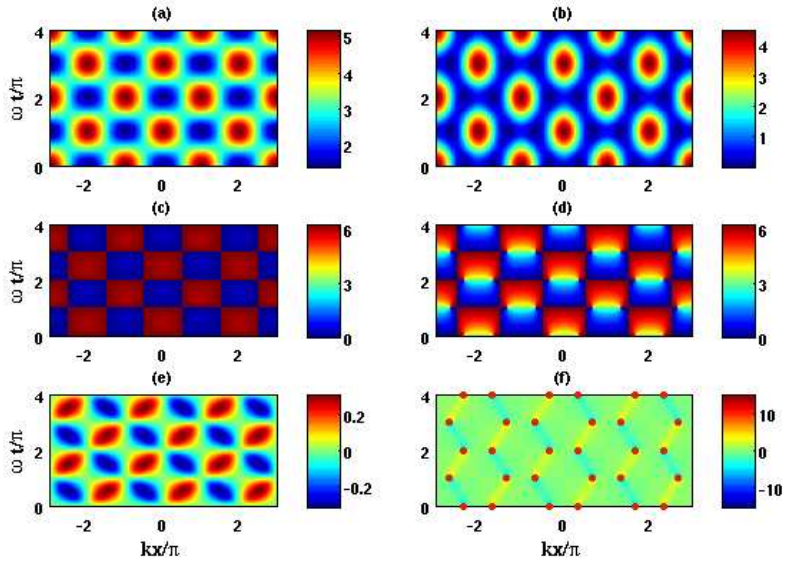

Figure 1. The spatiotemporal evolutions of the exact Floquet states: density evolutions (a) and (b), phase evolutions (c) and (d), and velocity evolutions (e) and (f). Left column [(a), (c) and (e)] corresponds to parameters $E_F/g_{1d} = 3k,\ V_0/g_{1d} = -0.3k,\ V_1/g_{1d} = 1.8974k$ in phase-continuing region $|V_1| > 2|V_0|$. Right column [(b), (d) and (f)] is associated with $E_F/g_{1d} = 0.5k,\ V_0/g_{1d} = -2k,\ V_1/g_{1d} = 2k$ in phase-jumping region $|V_1| < 2|V_0|$. The red dots in (f) are the points where phase jumps and velocity divergence occur. The atomic number-density R^2 is normalized in units of k, and the phase contribution from the factor $\exp(-\frac{i}{\hbar}E_F t)$ is eliminated.

$$\lim_{t\to t_n} R_t(x_{nl}^{\pm}, t) = V_1\omega_1/\sqrt{V_0},$$
$$\lim_{t\to t_n} R_{xx}(x_{nl}^{\pm}, t) \propto R^{-1}(x_{nl}^{\pm}, t_n) = \infty,$$
$$\lim_{t\to t_n} \theta_{xx}(x_{nl}^{\pm}, t) \propto R^{-1}(x_{nl}^{\pm}, t_n) = \infty.$$

With these formulas, one has

$$\lim_{t\to t_n} \psi_t(x_{nl}^{\pm}, t) \propto R_t(x_{nl}^{\pm}, t_n) = constant,$$

and

$$\lim_{t\to t_n} \psi_x(x_{nl}^{\pm}, t) \propto \theta_x(x_{nl}^{\pm}, t_n)R(x_{nl}^{\pm}, t_n) = constant.$$

Since $\psi,\ \psi_t$ and ψ_x are bounded, the phase-jump solution ψ is a bounded solution rather than a blowing-up one [29].

In Fig. 1, we show the spatiotemporal evolutions of the exact Floquet states for different parameters. The first, second and third rows show density, phase and velocity evolutions, respectively. The left and right columns have the parameters out and in region of phase jumps, respectively. For simplicity, without loss of generality, we rescale the density in units of k and eliminate the phase from the factor $\exp(-\frac{i}{\hbar}E_F t)$. It clearly shows that the phase-jump solution (right column) has nodes of zero density at which π phase jumps occur along the spatial direction and the corresponding velocities approach to infinite.

The nontrivial phase structure around the singular points, that is, the circulation integral $\oint(\theta_x dx + \theta_t dt) = \oint d\theta = 2n\pi$ $(n = 0, 1, 2\cdots)$ along closed spatiotemporal trajectories enclosing a singular point, reminds us the well-known Onsager-Feynman quantization condition for planar vortices [38, 39], since Eq. (16) implies that the integral around the spatiotemporal singular points is not equal to zero, and Eq. (10) allows the transformation $\theta \to \theta \pm n\pi$ at any spatiotemporal point. Therefore, mathematically, the circulation around the singular points turns out to be quantized as a consequence of the form of field $\theta(x,t)$. This means that the nonzero quantized integrals along the closed trajectories around the zero-density nodes indicate the existence of the $(1+1)$-D spatiotemporal vortex. Due to the analogues between the Floquet and Bloch analysis, the above Floquet states for an atomic BEC in 1D optical lattice with a spatiotemporal driving field are similar to the nonlinear Bloch modes in 2D periodic potentials [40], where the phase-jump solutions for the relatively weak driving strengthes correspond to the vortex solitons [41]. This peculiar type of vortices are called as spatiotemporal vortices [28]. Then the zero-density nodes $(x_{nl}^{\pm}, t_n)$ are vortex cores. From the phase distribution in the right column of Fig. 1, we find the phase accumulation along a circle around the vortex cores $(x_{nl}^{\pm}, t_n)$ is $\pm 2\pi$. This means that the vortex charge is ± 1 and so that the vortices at a pair of (x_{nl}^{+}, t_n) and (x_{nl}^{-}, t_n) are a vortex-antivortex pair.

4. Stability analysis and state preparation

In this section, we analyze the stability of the exact Floquet solution (4) for the nonlinear quantum system (1). In the sense of Lyapunov's stability, the instability entails that the initially small deviations grow in time without upper limit. Within the linear stability analysis [17, 16], the deviations are governed by the linearized equations for the unperturbed solution. If the linearized equations have any unbounded solution in time evolution, the corresponding unperturbed state is unstable. Only if all perturbed solutions are bounded, the unperturbed solution is stable. Usually, it is difficult to explore the stability of a nonstationary solution. However, it is relatively easy to show its instability. We will demonstrate that whether the nonlinear resonance from the velocity divergence can cause the dynamical instability.

The perturbations to the exact Floquet solution (4) can be taken in different forms. We consider the one of them, which has been used for stability analysis of stationary state solutions [17], in form of

$$\psi = [R(x,t) + \varepsilon\psi_1(x,t)] \exp[i\theta(x,t) - iE_F t/\hbar], \tag{18}$$

where the small parameter ε obeys $|\varepsilon| \ll 1$ and the perturbation correction $\psi_1(x,t) = \phi(x,t) + i\varphi(x,t)$ including a real part ϕ and an imaginary part φ. According to the linear stability analysis, the Lyapunov stability of solution requires that the unperturbed and perturbed solutions satisfy the spatially boundary conditions and all first-order corrections including $||\psi_1|| = \sqrt{|\phi|^2 + |\varphi|^2}$ for arbitrarily boundary conditions are bounded in the time evolution, and the Lyapunov instability is associated with the

unboundedness of any perturbed solution. Substituting the perturbed solution (18) into the original equation (1), we get the linearized equations

$$\hbar\phi_t = L_1\varphi - S\phi, \tag{19}$$

$$\hbar\varphi_t = -(L_3\phi + S\varphi), \tag{20}$$

where the operators L_j and S satisfy[17]

$$L_j = -\frac{\hbar^2}{2m}\Big[\frac{\partial^2}{\partial x^2} - \theta_x^2(x,t)\Big] + jg_{1d}R^2(x,t) + V(x,t) + \hbar\theta_t(x,t), (for\ j = 1\ and\ 3), \tag{21}$$

$$S = \frac{\hbar^2}{2m}\Big[2\theta_x(x,t)\frac{\partial}{\partial x} + \theta_{xx}(x,t)\Big]. \tag{22}$$

Using these operators and the relation $\psi = R\exp(i\theta)$, we can rewrite the unperturbed system (1) as $L_1R = 0$ and $\hbar R_t + SR = 0$.

From the linearized equations (19)-(22), we know that the bounded solutions ϕ and φ must be zero at the zero-density nodes $(x_{nl}^{\pm}, t_n)$ which are singular points of θ_x and θ_{xx}. It is quite difficult to solve the perturbed equations (19) and (20) for ϕ and φ. However, we can show the instability from the singularity of first derivatives ϕ_t and φ_t. Mathematically, the linearized equations (19) and (20) are a couple of partially differential equations with general solutions containing some arbitrary functions, which are associated with various initial perturbations. For the solutions of spatiotemporal vortices, the linearized equations (19) and (20) are singularly differential equations with infinite θ_x and θ_{xx} at the zero-density nodes $(x_{nl}^{\pm}, t_n)$. Perhaps one may find a set of special solutions for the linearized equations (19) and (20) whose first time derivatives ϕ_t and φ_t are bounded. Nevertheless, since $\phi(x_{nl}^{\pm}, t_n)$ and $\varphi(x_{nl}^{\pm}, t_n)$ cannot keep vanished for the arbitrary functions included in the general solutions $\phi(x,t)$ and $\varphi(x,t)$, we cannot guarantee the boundedness of the first time derivatives in the singular Eqs. (19) and (20). Hence, under some initial perturbations the singularity of $\theta_x(x_{nl}^{\pm}, t_n)$ and $\theta_{xx}(x_{nl}^{\pm}, t_n)$ will result in the divergence of $\phi_t(x_{nl}^{\pm}, t_n)$ and $\varphi_t(x_{nl}^{\pm}, t_n)$. That is, the linearized equations (19) and (20) have blowing-up solutions [29] in the phase-jump region which supports trains of spatiotemporal vortex-antivortex pairs. The blowing-up of the perturbed solutions could break down the integrability of linearized equations (19) and (20) and induce the jumps in $\phi(x_{nl}^{\pm}, t_n)$ and $\varphi(x_{nl}^{\pm}, t_n)$. Moreover, the jumping heights $\triangle\phi(x_{nl}^{\pm}, t_n)$ and $\triangle\varphi(x_{nl}^{\pm}, t_n)$ may be uncontrollably large, because of the non-integrability of the linearized equations (19) and (20) and the singularities of $\theta_x^2(x,t)\phi(x,t)$ and $\theta_x^2(x,t)\varphi(x,t)$ at the vortex cores $(x_{nl}^{\pm}, t_n)$. Therefore, the blowing-up of perturbed solutions relates to the instability of the system.

To confirm the above theoretical analysis for instability, we numerically integrate the GP equation (1) with the well-developed operator-splitting method. In our numerical simulation, we input the initial conditions as the initial values of the corresponding exact Floquet states and choose the same parameters used in Fig. 1 and the periodic boundary conditions $\psi(x_{max}, t) = \psi(-x_{max}, t)$ of $x_{max} = 4$. To show the difference between the exact Floquet solution and the numerical one, we calculate the

time evolution of fidelity $F(t)$ between the exact solution $\psi_{ex}(x,t)$ without perturbations and the numerical one $\psi_{num}(x,t)$ with initial white noise,

$$F(t) = \frac{1}{N_C(t)} \left| \int \psi^*_{num}(x,t)\psi_{ex}(x,t)dx \right|^2, \tag{23}$$

where the normalization function is defined as

$$N_C(t) = \int \psi^*_{num}(x,t)\psi_{num}(x,t)dx \times \int \psi^*_{ex}(x,t)\psi_{ex}(x,t) \qquad dx, \tag{24}$$

which ensures the fidelity satisfying $0 \leq F(t) \leq 1$. Here, the functions $\psi^*_{ex}(x,t)$ and $\psi^*_{num}(x,t)$ stand for the complex conjugates of functions $\psi_{ex}(x,t)$ and $\psi_{num}(x,t)$. Due to the GP system (1) conserves the total number of atoms, we have $N_C(t) = N_C(0)$. The fidelity describes the similarity between the two solutions, $F = 1$ means the two solutions are the same and $F = 0$ means no similarity between them. So the fast decay of fidelity indicates that the initially small deviation from the unperturbed state grows fast. This is a signature for the instability of a quantum evolution [31, 32].

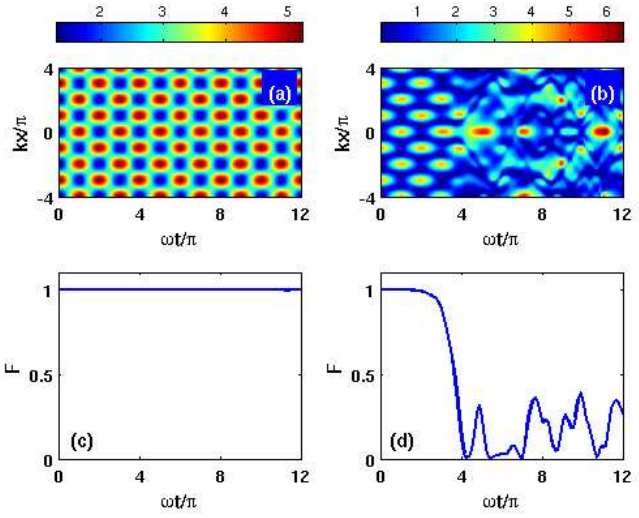

Figure 2. The numerical evolutions for the same cases shown in Fig. 1. The left [(a) and (c)] and right [(b) and (d)] columns have the same parameters with the left and right columns of Fig. 1, respectively. The above [(a) and (b)] and below [(c) and (d)] rows show the density and fidelity evolutions, respectively. For the non-vortex state (left column) the density evolution is regular and periodic, and the fidelity perfectly keeps close to one. But for the solution of spatiotemporal vortices (right column) after a short period of time the density evolution becomes chaotic and the fidelity shows fast decay, which is a signature of instability.

In Fig. 2, we show the numerical simulations correspond to the exact evolutions shown in Fig. 1. For the non-vortex solutions (left column), the density evolution from numerical simulation is regular and periodic, and the fidelity between the numerical and exact solutions perfectly keeps close to one. This means that the two solutions are

almost the same and the exact Floquet state maintains its stability under the numerical perturbation. For the solution of spatiotemporal vortices, the density evolution becomes chaotic after a short period of time, and the corresponding fidelity quickly decays to zero after a short period of time and then chaotically oscillates around a small number close to zero. This means the spatiotemporal vortices being the periodic state embedded in chaos and indicates the system losing its stability under the numerical perturbation. In order to avoid such an instability, we need adjust the driving field strength $|V_1|$ and lattice depth V_0 to satisfy $|V_1| \geq 2|V_0|$. Due to the instability is related to the nonlinear resonance, we call such an instability as the nonlinear resonance instability.

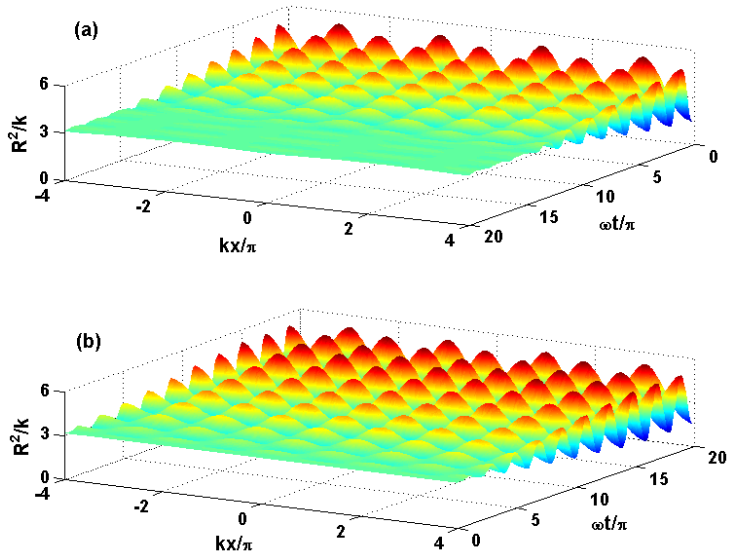

Figure 3. State transition and preparation via slow varying processes. (a) Transition from a stable Floquet state to a uniform state by slowly ramping down the external potential $V(x,t) = A(t)[\cos^2 kx + (V_1/V_0)\cos kx \cos \omega t]$ from $A = V_0$ to $A = 0$ and then keeping A as zero. (b) Preparation of a stable Floquet state from an uniform state of density $R^2(x) = \mu/g_{1d}$ with $\mu = E_F - V_0/2$ and phase $\theta(x) = \theta_0$ by slowly ramping up the external potential $V(x,t) = A(t)[\cos^2 kx + (V_1/V_0)\cos kx \cos \omega t]$ from $A = 0$ to $A = V_0$ and then keeping A as V_0. In which, the values of V_0, V_1, E_F, k and ω are as same as the ones for (a) of Fig. 1, and the linear ramping processes occur in the period from $t = 0$ to $t = 15\pi/\omega$ and then the amplitude A keeps unchanged after $t = 15\pi/\omega$.

The numerical and analytical results show that the condensate in the non-stationary states is stable in the parameter region $|V_1| \geq 2|V_0|$, $V_0 \leq V_c/3$. Noting the balance condition $|V_1| = 2\sqrt{|E_F V_0|}$ and the average number of atoms per well $N = \pi(|E_F| + |V_0|/2)/(k|g_{1d}|)$, for a fixed N the Floquet energy E_F is controlled by the driving field strength V_1 and lattice depth V_0. Therefore, one can control the oscillation amplitude and flow density of the stable Floquet states by adjusting the driving field strength and lattice depth. To precisely prepare the Floquet states analyzed above, one can use the similar techniques of adiabatic growth which has been successfully used to prepare stationary states for systems of time-independent potentials [13]. However, due

to our penitential is time-dependent even ignoring the time-dependence of the amplitude, the slow varying processes used here is non-adiabatic. Because of the conserved total particle number, the state $\psi = Re^{-i\mu t}$ of uniform density distribution $R^2(x) = \mu/g_{1d}$ with $\mu = E_F - V_0/2$ and trivial phase distribution $\theta(x) = \theta_0$ (θ_0 is a constant determined by initial conditions) can be obtained by slowly ramping down the external potential $V(x,t) = A(t)[\cos^2 kx + (V_1/V_0)\cos kx \cos \omega t]$ from $A = V_0$ to $A = 0$. Inversely, from the uniform state of density $R^2(x) = (E_F - V_0/2)/g_{1d}$ and trivial phase, one can get the exact Floquet state (4) for the stability region $|V_1| \geq 2|V_0|$, $V_0 \leq V_c/3$ by slowly ramping up the external potential $V(x,t) = A(t)[\cos^2 kx + (V_1/V_0)\cos kx \cos \omega t]$ from $A = 0$ to $A = V_0$.

In Fig. 3, we show our numerical simulation for the state transition and preparation via slow varying processes. For convenience, we choose the same values of V_0, V_1, E_F, k and ω for (a) of Fig. 1, which describes a stable Floquet state. In panel (a), whose external potential is linearly ramped down from $A = V_0$ to $A = 0$, we show the density evolution of a condensate evolving from the stable Floquet state [which is shown in panel (a) of Fig. 1] to an uniform state. Accompanying with the decrease of $|A|$, the density difference between different positions becomes smaller and smaller. After $t = 15\pi/\omega$, there is no external potential, the density $R^2/k = (E_F - V_0/2)/(kg_{1d}) \pm 0.1 = 3.15 \pm 0.1$. This means that the relative density difference $\Delta(R^2)/\langle R^2 \rangle$ is about 3%. The fidelity between the final state and the corresponding exact uniform state is above 98%. In panel (b), whose external potential is linearly ramped up from $A = 0$ to $A = V_0$, we show the density evolution of a condensate evolving from the state of uniform density $R^2(x) = (E_F - V_0/2)/g_{1d}$ and trivial phase to a stable Floquet state. Accompanying with the growth of $|A|$, the density oscillation becomes more and more close to the one of the exact Floquet state. After $t = 15\pi/\omega$, the fidelity between the prepared state and the exact Floquet state for the corresponding parameters is also above 98%. The numerical results may supply a useful benchmark for preparing and manipulating the stable Floquet states in experiments.

5. Conclusions and discussions

In conclusion, for an atomic BEC in a one-dimensional optical lattice, we have shown how to prepare the exactly nonlinear Floquet states in a balance parametric region via a spatiotemporally periodic driving field. The exact Floquet solution describes the interference between an atomic standing wave and an uniform background. The balance condition requires that the sum of internal and external potentials is equal to the Floquet energy which is proportional to the atomic number per well and the depth of the lattice potential. It is shown that the phase of the exact Floquet solution may be continuous or piecewise continuous, depending on the ratio between the driving intensity and lattice depth. The phase-jumping solutions with piecewise continuous phase include the trains of spatiotemporal vortex-anitvortex pairs which are embedded in chaos. Applying the linear stability analysis, we have analyzed the stability and instability of the exact

Floquet states. The instability is related to the blowing-up of the perturbed solutions and the nonlinear resonance. The stable periodic states and unstable phase-jumping states have been numerically illustrated by the corresponding fidelities between the analytically unperturbed solution and the numerically perturbed solution. Dividing the balance region of parameters into the stability and instability subregions, we can selectively prepare the stable periodic states and unstable spatiotemporal vortex states by adjusting the driving strength and lattice depth to fit the corresponding subregions, and prepare the different stationary states by adiabatically switching off the driving field.

We expect the above exact Floquet states in nonlinear quantum systems would stimulate experimental interests in investigating and stabilizing the non-stationary and stationary condensates. It would be helpful to explore the chaotic dynamics in such non-integrable systems of spatiotemporal periodic potentials like $V(x,t)$ [35, 34]. For the non-integrable system of driven condensates, the exact Floquet state is completely determined by the parameters of external field. Therefore, we can prepare and control the spatiotemporal structures described by the Floquet solutions via choosing and adjusting parameters in the balance region. For a small ratio between the driving intensity and lattice depth one could explore the instability from velocity singularity via observing the breakdown of the periodic structure in density distribution [42, 19]. Utilizing the slow varying processes, one can selectively prepare the stable Floquet states. Particularly, the results points out a general route to experimentally stabilizing and preparing the non-stationary states of the condensate.

Additionally, with the similarity between the Floquet and Bloch analysis, the well-developed techniques for manipulating the atomic condensates with laser and magnetic fields offer an opportunity to study the analogue and difference between Floquet states and Bloch modes including spatial and spatiotemporal vortices.

Acknowledgment – The authors thank Prof. Yuri S. Kivshar for stimulating discussions and valuable suggestions. This work was supported by the National Natural Science Foundation of China under Grant No. 10575034, and the Australian Research Council (ARC).

References

[1] Fölling F, Gerbier F, Widera A, Mandel O, Gericke T and Bloch I, 2005 Nature **434**, 481.
[2] Anderson B P and Kasevich M A, 1998 Science **282**, 1686.
[3] Orzel C, Tuchman A K, Fenselau M L, Yasuda M, and Kasevich M A, 2001 Science **291**, 2386.
[4] Lee C, Alexander T J, and Kivshar Yu S, 2006 Phys. Rev. Lett. **97**, 180408; Lee C, 2004 Phys. Rev. Lett. **93**, 120406.
[5] Liu W M, Fan W B, Zheng W M, Liang J Q, Chui S T, 2002 Phys. Rev. Lett. **88**, 170408.
[6] Chong G, Hai W and Xie Q, 2005 Phys. Rev. E **71**, 016202.
[7] Ostrovskaya E A and Kivshar Yu S, 2004 Phys. Rev. Lett. **93**, 160405.
[8] Pachos J K and Knight P L, 2003 Phys. Rev. Lett. **91**, 107902.
[9] Ionicioiu R and Zanardi P, 2002 Phys. Rev. A **66**, 050301(R).
[10] Lee C and Ostrovskaya E A, 2005 Phys. Rev. A **72**, 062321.

[11] Ovchinnikov Yu B, Müller J H, Doery M R, Vredenbregt E J D, Helmerson K, Rolston S L, and Phillips W D, 1999 Phys. Rev. Lett. **83**, 284.
[12] Choi D I and Niu Q, 1999 Phys. Rev. Lett. **82**, 2022.
[13] Bronski J C, Carr L D, Deconinck B, and Kutz J N, 2001 Phys. Rev. Lett. **86**, 1402.
[14] Deconinck B, kutz J N, Patterson M S, and Warner B W, 2003 J. Phys. A **36**, 5431.
[15] Hai W, Li Y, Xia B, and Luo X, 2005 Europhys. Lett. **71**, 28.
[16] Wu B and Niu Q, 2001 Phys. Rev. A **64**, 061603(R).
[17] Bronski J C, Carr L D, Deconinck B, Kutz J N, and Promislow K, 2001 Phys. Rev. E **63**, 036612.
[18] Ruprecht P A, Edwards M, Burnett K, and Clark C W, 1996 Phys. Rev. A **54**, 4178.
[19] Fallani L, Sarlo L De, Lye J E, Modugno M, Saers R, Fort C, and Inguscio M, 2004 Phys. Rev. Lett. **93**, 140406.
[20] Bradley R M, Deconinck B and Nathan J Kutz, 2005 J. Phys. A: Math. Gen. **38** 1901.
[21] Deng H, Hai W and Zhu Q, 2006 J. Phys. A: Math. Gen. **39**, 15061.
[22] Holthaus M, Chaos, 2001 Phys. Rev. A **64**, 011601R.
[23] Xie Q and Hai W, 2007 Phys. Rev. A **75**, 015603.
[24] Eckardt A, Weiss C, and Holthaus M, 2005 Phys. Rev. Lett. **95**, 260404.
[25] Pismen L M, *Vortices in Nonlinear Fields* (Clarendon Press, Oxford, 1999), p. 290.
[26] Soskin M S and Vasnetsov M V, in *Progress in Optics*, edited by Wolf E (North-Holland, Amsterdam, 2001), Vol. **42**, p. 219.
[27] Madison K W, Chevy F, Wohlleben W, and Dalibard J, 2000 Phys. Rev. Lett. **84**, 806; Raman C, Abo-Shaeer J R, Vogels J M, Xu K, and Ketterle W, 2001 Phys. Rev. Lett. **87**, 210402.
[28] Sukhorukov A P and Yangirova V V, 2005 Proc. SPIE 5949, 594906.
[29] For an example, see Guo B and Pang X, *Solitons*, (Science Press, Beijing, p243, 1987) (in Chinese), and references there in.
[30] Konotop V V and Pacciani P, 2005 Phys. Rev. Lett. **94**, 240405.
[31] Peres A, 1984 Phys. Rev. A **30**, 1610.
[32] Gorin T, Prosen T, Seligman T H, and Znidaric M, 2000 Phys. Rep. **435**, 33.
[33] Abdullaev F Kh and Galimzyanov R, 2003 J. Phys. B: At. Mol. Opt. Phys. **36**, 1099
[34] Bishop S R, Clifford M J, 1996 J. Sound Vib. **189**, 142.
[35] Hensinger W K, Heckenberg N R, JMilburn G and Rubinsztein-Dunlop H, 2003 J. Opt. B: Quantum Semiclass. Opt. **5**, R83.
[36] Yang J and Jing Z, 2008 Chaos, Solitons and Fractals **35**, 726.
[37] Adhikari S K, 2003 J. Phys. B: At. Mol. Opt. Phys. **36** 1109.
[38] Onsager L, 1949 Nuovo Cimento Suppl. **6**, 249.
[39] Penn V, 1999 Phys. Rev. B **59**, 7127.
[40] Träger D, Fischer R, Neshev D N, Sukhorukov A A, Denz C, Królikowski W, and Kivshar Yu S, 2006 Opt. Express **14**, 1913.
[41] Alexander T J, Desyatnikov A S, and Kivshar Yu S, 2007 Opt. Lett. **32**, 1293.
[42] Strekalov D V, Turlapov A, Kumarakrishnan A, and Sleator T, 2002 Phys. Rev. A **66**, 023601.